Corrections

CELL BIOLOGY

Correction for "Dysregulation of PAD4-mediated citrullination of nuclear GSK3β activates TGF-β signaling and induces epithelial-to-mesenchymal transition in breast cancer cells," by Sonja C. Stadler, C. Theresa Vincent, Victor D. Fedorov, Antonia Patsialou, Brian D. Cherrington, Joseph J. Wakshlag, Sunish Mohanan, Barry M. Zee, Xuesen Zhang, Benjamin A. Garcia, John S. Condeelis, Anthony M. C. Brown, Scott A. Coonrod, and C. David Allis, which appeared in issue 29, July 16, 2013, of *Proc Natl Acad Sci USA* (110:11851–11856; first published July 1, 2013; 10.1073/pnas.1308362110).

The authors note that the affiliation for C. Theresa Vincent should also include [k]Cell and Developmental Biology, Weill Cornell Medical College, New York, NY 10065. The corrected author and affiliation lines appear below. The online version has been corrected.

Sonja C. Stadler[a,b], C. Theresa Vincent[c,d,k], Victor D. Fedorov[e], Antonia Patsialou[f], Brian D. Cherrington[g], Joseph J. Wakshlag[h], Sunish Mohanan[i], Barry M. Zee[j], Xuesen Zhang[i], Benjamin A. Garcia[j], John S. Condeelis[f], Anthony M. C. Brown[k], Scott A. Coonrod[i], and C. David Allis[a]

[a]Laboratory of Chromatin Biology and Epigenetics, The Rockefeller University, New York, NY 10065; [b]Institute of Laboratory Medicine, Clinical Chemistry, and Molecular Diagnostics and LIFE Leipzig Research Center for Civilization Diseases, University of Leipzig, 04103 Leipzig, Germany; Departments of [c]Physiology and Biophysics and [k]Cell and Developmental Biology, Weill Cornell Medical College, New York, NY 10065; [d]Department of Medicine, Center for Molecular Medicine, Karolinska Institutet, 171 76 Stockholm, Sweden; [e]Center for Cell Engineering, Molecular Pharmacology and Chemistry Program, Memorial Sloan-Kettering Cancer Center, New York, NY 10065; [f]Department of Anatomy and Structural Biology, Albert Einstein College of Medicine, Bronx, NY 10461; [g]Department of Zoology and Physiology, University of Wyoming, Laramie, WY 82071; [h]Department of Clinical Sciences and [i]Baker Institute for Animal Health, College of Veterinary Medicine, Cornell University, Ithaca, NY 14853; and [j]Department of Biochemistry and Biophysics, Perelman School of Medicine, University of Pennsylvania, Philadelphia, PA 19104

www.pnas.org/cgi/doi/10.1073/pnas.1315590110

MEDICAL SCIENCES

Correction for "*BRCA1* promotes the ubiquitination of PCNA and recruitment of translesion polymerases in response to replication blockade," by Fen Tian, Shilpy Sharma, Jianqiu Zou, Shiaw-Yih Lin, Bin Wang, Khosrow Rezvani, Hongmin Wang, Jeffrey D. Parvin, Thomas Ludwig, Christine E. Canman, and Dong Zhang, which appeared in issue 33, August 13, 2013, of *Proc Natl Acad Sci USA* (110:13558–13563; first published July 30, 2013; 10.1073/pnas.1306534110).

The authors note that they omitted a reference to an article by Pathania et al. The complete reference appears below.

Furthermore, the authors note that "It is important to note that the role of *BRCA1* in response to UV induced replication stress has also been examined by Livingston and colleagues (41). Both studies observed some overlapping phenotypes in *BRCA1* depleted cells (for example, the reduction of RPA foci when treated with UV). However, the two studies also have some discrepancies with respect to PCNA ubiquitination. We speculate that these discrepancies may be due to the knockdown efficiency of *BRCA1*."

41. Pathania S, et al. (2011) BRCA1 is required for postreplication repair after UV-induced DNA damage. *Mol Cell* 44(2):235–251.

www.pnas.org/cgi/doi/10.1073/pnas.1316463110

PLANT BIOLOGY

Correction for "Dirigent domain-containing protein is part of the machinery required for formation of the lignin-based Casparian strip in the root," by Prashant S. Hosmani, Takehiro Kamiya, John Danku, Sadaf Naseer, Niko Geldner, Mary Lou Guerinot, and David E. Salt, which appeared in issue 35, August 27, 2013, of *Proc Natl Acad Sci USA* (110:14498–14503; first published August 12, 2013; 10.1073/pnas.1308412110).

The authors note that the contributions line appeared incorrectly. The corrected author contributions footnote appears below.

P.S.H., T.K., N.G., M.L.G., and D.E.S. designed research; P.S.H., T.K., J.D., and S.N. performed research; P.S.H., T.K., J.D., S.N., N.G., M.L.G., and D.E.S. analyzed data; and P.S.H. and D.E.S. wrote the paper.

www.pnas.org/cgi/doi/10.1073/pnas.1315919110

Dirigent domain-containing protein is part of the machinery required for formation of the lignin-based Casparian strip in the root

Prashant S. Hosmani[a], Takehiro Kamiya[b], John Danku[b], Sadaf Naseer[c], Niko Geldner[c], Mary Lou Guerinot[a], and David E. Salt[b,1]

[a]Department of Biological Sciences, Dartmouth College, Hanover, NH 03755; [b]Institute of Biological and Environmental Sciences, University of Aberdeen, Aberdeen AB24 3UU, United Kingdom; and [c]Department of Plant Molecular Biology, University of Lausanne–Sorge, 1015 Lausanne, Switzerland

Edited by Philip N. Benfey, Duke University, Durham, NC, and approved July 22, 2013 (received for review May 7, 2013)

The endodermis acts as a "second skin" in plant roots by providing the cellular control necessary for the selective entry of water and solutes into the vascular system. To enable such control, Casparian strips span the cell wall of adjacent endodermal cells to form a tight junction that blocks extracellular diffusion across the endodermis. This junction is composed of lignin that is polymerized by oxidative coupling of monolignols through the action of a NADPH oxidase and peroxidases. Casparian strip domain proteins (CASPs) correctly position this biosynthetic machinery by forming a protein scaffold in the plasma membrane at the site where the Casparian strip forms. Here, we show that the dirigent-domain containing protein, enhanced suberin1 (ESB1), is part of this machinery, playing an essential role in the correct formation of Casparian strips. ESB1 is localized to Casparian strips in a CASP-dependent manner, and in the absence of ESB1, disordered and defective Casparian strips are formed. In addition, loss of ESB1 disrupts the localization of the CASP1 protein at the casparian strip domain, suggesting a reciprocal requirement for both ESB1 and CASPs in forming the casparian strip domain

The root is the central plant organ required for water and mineral nutrient uptake from the soil. Understanding the mechanisms underlying root function is therefore central for developing plants with the improved root systems required for the more efficient water and mineral nutrient utilization needed to drive sustainable increases in food production and quality. The rate limiting step in water and mineral nutrient transport to the shoot is radial transport across the root (1). Radial transport involves movement of water and dissolved solutes from the soil, through the epidermis, cortex, and endodermal cell layers and into the vascular system (1). Transport occurs through the cell wall continuum (apoplasm) or cell to cell by using symplastic or transmembrane pathways. The differentiation of the endodermis is marked by the formation in the cell wall of the Casparian strip, a belt-like structure surrounding the cell and running parallel to the root surface in the anticlinal cell wall. This structure is composed of a fine band of lignin (2) tightly adhered to the plasma membrane and spanning the apoplastic space between adjacent endodermal cells. Casparian strips form a physical barrier to extracellular diffusion (3, 4), allowing endodermal cells to exert control over passage of water and solutes into the stele and the vascular system for transport throughout the plant (5). Lignin-forming Casparian strips is polymerized by oxidative coupling of monolignols through the action of specific localized NADPH oxidase and peroxidases (6). The Casparian strip membrane domain proteins (CASPs) (7) form a protein scaffold at the Casparian strip domain, the region of the plasma membrane where the Casparian strip will form. This scaffold is thought to be involved in correctly positioning the biosynthetic machinery involved in building the Casparian strip. However, the proteins required for the precise control of lignin deposition to a fine band spanning the cell wall between adjacent endodermal cells to form the Casparian strip are unknown.

Results and Discussion

Enhanced suberin1 (*ESB1*) was originally identified in a forward genetic screen of *Arabidopsis thaliana* for mutants with altered mineral nutrient and trace element contents (8, 9). The *esb1* mutant displays changes in the leaf accumulation of various elements, including a significant reduction in calcium, which are proposed to be caused by the observed increase of suberin deposition in the roots of this mutant (8, 10). *ESB1* encodes a protein containing a predicted 154-aa residue dirigent domain (Pfam 26.0 PF03018) (11). Dirigent proteins have been characterized to act as nonenzymatic templates guiding bond formation between two monolignols to define the stereochemistry of the resulting dimeric lignin (12). It has been suggested that dirigent proteins can guide synthesis of lignin by providing a template for a specific order of monolignol subunits during lignin deposition in the cell wall (13), but these observations need to be reconciled with biochemical evidence that lignin polymerization can occur in the absence of proteinaceous control (14). Here, we demonstrate that the dirigent domain containing protein ESB1 is required for the correct patterning of lignin deposition in Casparian strips. Use of a stably expressed protein fusion of ESB1 with red fluorescent mCherry under the transcriptional control of the *ESB1* native promoter revealed that *ESB1* is uniquely expressed in the endodermis (Fig. 1 *A*–*C*) and localizes in a band-like structure around the endodermal cells in a similar pattern to Casparian strips (Fig. 1 *D* and *E*). Interestingly, ESB1-mCherry appears to initially localize along the equatorial line of the endodermal cell in patches, which then coalesce to form

Significance

The endodermis acts as a "second skin" in plant roots by providing the cellular control necessary for the selective entry of water and mineral nutrients into the vascular system. To enable such control, Casparian strips span the cell wall of adjacent endodermal cells to form a tight junction that blocks diffusion across the endodermis in the cell wall. This junction is composed of a fine band of lignin, the polymer that gives wood its strength. Here, we characterize a dirigent protein (from Latin, *dirigere*: to guide or align) as playing a vital role in the patterning of lignin in the Casparian strip, identifying a new component of the molecular machinery that builds Casparian strips.

Author contributions: D.E.S. designed research; P.S.H., T.K., J.D., and S.N. performed research; N.G. contributed new reagents/analytic tools; P.S.H., T.K., J.D., S.N., N.G., M.L.G., and D.E.S. analyzed data; and P.S.H. and D.E.S. wrote the paper.

The authors declare no conflict of interest.

This article is a PNAS Direct Submission.

Freely available online through the PNAS open access option.

[1]To whom correspondence should be addressed. E-mail: david.salt@abdn.ac.uk.

This article contains supporting information online at www.pnas.org/lookup/suppl/doi:10.1073/pnas.1308412110/-/DCSupplemental.

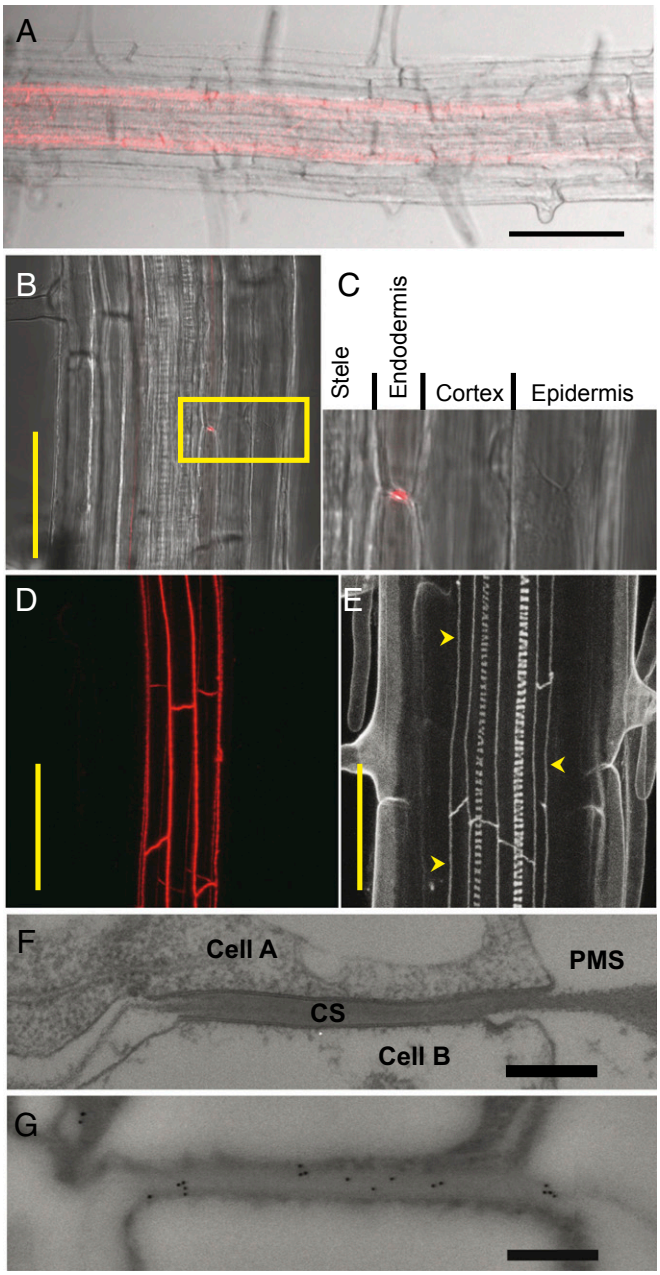

Fig. 1. The dirigent domain containing protein ESB1 accumulates uniquely in the root endodermis at the Casparian strips. (*A–D*) *ESB1-mCherry* expression from native *ESB1* promoter in roots of *esb1-1*. Confocal image (red) merged with transmission image (*A–C*). (*C*) Enlargement of area boxed in *B*. (*D*) *Z*-stack confocal image (red) in the same area as *B*. (*E–G*) Casparian strips in wild-type roots. (*E*) *Z*-stack confocal image of lignin autofluorescence (arrows indicate Casparian strips). (*F*) Transmission electron micrograph of a representative Casparian strip. (*G*) Representative image of immunogold-electron micrograph at the anticlinal wall of an endodermal cell by using anti-ESB1 antibodies. CS, Casparian strip; PMS, space generated by plasmolysis. (Scale bars: *A*, 100 μm; *B*, *D*, and *E*, 50 μm; *F* and *G*, 500 nm.)

a continuous band (Fig. 2). This ESB1-mCherry localization process is similar to that previously observed for CASP1-GFP (7) and for the deposition of the Casparian strip (6), which both pass through a patchy stage before coalescing into continuous strips. Immunogold electron microscopy confirmed that native ESB1 protein is specifically localized to the Casparian strip (Fig. 1 *F* and *G*), and this localization was lost in *esb1-1* (Fig. S1*A*). Significantly, ESB1 localization to the Casparian strip requires CASPs because immunogold labeling of ESB1 at the Casparian strip is reduced in the *casp1-1casp3-1* double mutant (Fig. S1*A*). Further, in the *casp1-1casp3-1* mutant, immunogold particles specific for ESB1 appear to accumulate in the cytoplasm (Fig. S1*B*), supporting the mistargeting of ESB1 in this double mutant.

Loss of *ESB1* function in *esb1-1* causes a complete loss of the well-organized structure of Casparian strips as revealed by electron microscopy (Fig. 3 *A* and *B*). Confocal imaging of Casparian strips using autofluorescence confirms this malformation (Fig. 3 *D* and *E*). The Casparian strips of wild-type endodermal cell walls are replaced in *esb1-1* with deposition of fluorescent material in patches in the equatorial region of the endodermal cells, and also in the corners of the cells on both the cortex and pericycle faces (Fig. 3 *D* and *E* and Movie S1). Raman confocal microscopy (15) establishes that the disrupted Casparian strips in *esb1-1* are composed of an enhanced deposition of lignin-like material with a similar chemical composition to wild-type Casparian strips and xylem lignin (Fig. 4). This disrupted Casparian strip morphology is fully complemented by expression of wild-type *ESB1* or an *ESB1-mCherry* construct from the native *ESB1* promoter (Figs. S2*A* and S3*A*). Propidium iodide (PI) is a fluorescent dye used as an apoplastic tracer whose movement into the inner cell layer of the stele is blocked by Casparian strips (2). Staining with PI revealed that *esb1-1* shows delayed barrier development (Fig. 3 *G* and *H*) that is complemented by expression of wild-type *ESB1* from its native promoter (Fig. S2 *B* and *C*). The enhanced deposition of lignin in *esb1-1* could be explained in several different ways. In the

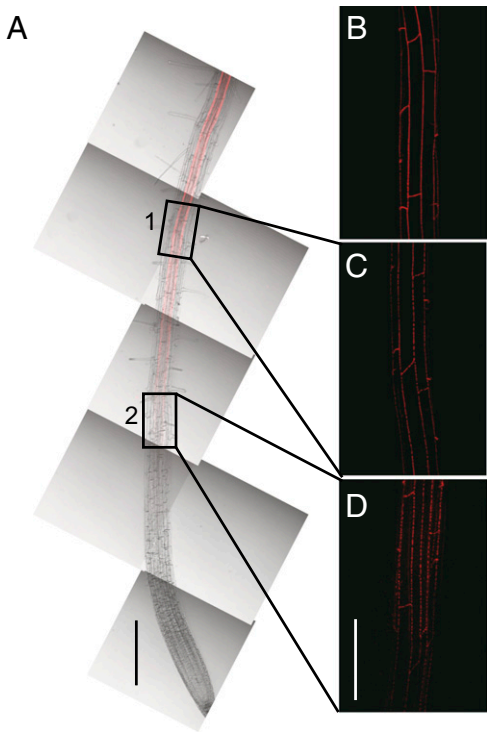

Fig. 2. The dirigent domain containing protein ESB1 localized at the endodermis in equatorially located patches that coalesce into a continuous strip. (*A–D*) *ESB1-mCherry* expression in *esb1-1* transgenic plants were grown for 6 d, and mCherry fluorescence was observed by confocal microscope. (*A*) ESB1-mCherry observed in a 5-mm section of root. Confocal image (red) was merged with transmission image, and multiple merged images were tiled to form a combined image. Higher magnification *Z*-stack confocal images taken 6 mm from the root tip (*B*), in boxed area 1 (*C*), and in boxed area 2 (*D*). (Scale bars: *A*, 500 μm; *B–D*, 100 μm.)

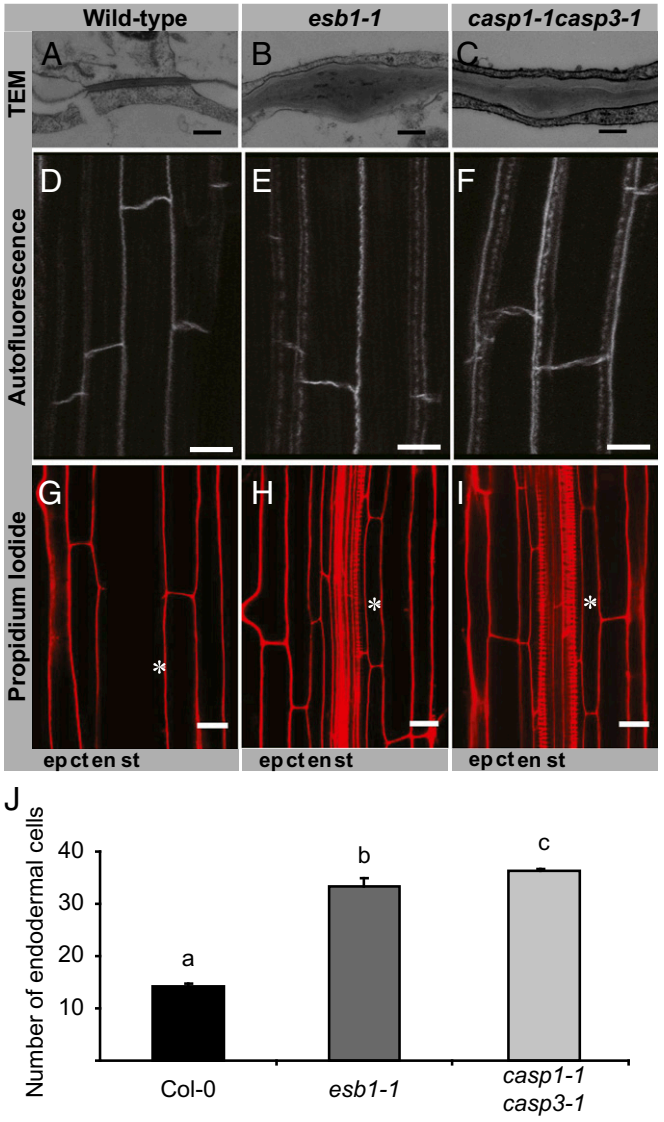

Fig. 3. The dirigent-domain protein ESB1 is required for the normal morphology and function of the lignin Casparian strip. Transmission electron micrographs showing Casparian strip in wild-type (*A*), *esb1-1* (*B*), and *casp1-1casp3-1* (*C*). Autofluorescence visualization after clearing root in wild-type (*D*), *esb1-1* (*E*), and *casp1-1casp3-1* (*F*). PI penetration in wild-type (*G*), *esb1-1* (*H*), and *casp1-1casp3-1* (*I*). Asterisks mark the 30th endodermal cell after onset of elongation. Onset of elongation is defined as the zone where the length of an endodermal cell was observed to be more than twice its width. (*J*) Quantification of PI penetration into the stele quantified as number of endodermal cells from the first fully expanded cell in wild-type, *esb1-1*, and *casp1-1casp3-1*. Casparian strips in wild-type plants form a barrier to apoplastic diffusion of PI starting at the 13th endodermal cell from the onset of elongation, whereas in *esb1-1*, this barrier does not form until the 32nd endodermal cell. Different letters (a, b, and c) indicate statistically significant differences between means by one-way analysis of variance (ANOVA) with Tukey–Kramer separation of means ($P < 0.05$), $n = 15$ roots. (Scale bars: *A*–*C*, 250 nm; *D*–*F*, 10 μm; *G*–*I*, 20 μm.) ct, cortex; en, endodermis; ep, epidermis; st, stele.

absence of ESB1, it is possible that polymerization of monolignols, usually directed by localized NADPH oxidases and peroxidases (6), does not proceed normally, as indicated by the islands of lignin observed in *esb1-1*. Unpolymerized monolignols could accumulate in the corners of the cells where they are activated by nonspecific peroxidase and polymerize to form ectopic lignin deposits. This process would occur in an unregulated manner, forming a sink for monolignols and allowing increased levels of lignin to accumulate. It is also possible that to repair the disrupted Casparian strip in *esb1-1*, release of monolignols into the cell wall is stimulated, providing substrate for enhanced lignifications. In *esb1-1* the development of an effective barrier to apoplastic diffusion of PI at the endodermis is delayed but not completely blocked. A functional barrier develops in more mature endodermal cells (30 cells from the root tip) (Fig. 3*J*), supporting the idea that the enhanced lignification observed in *esb1-1* is a Casparian strip repair mechanism.

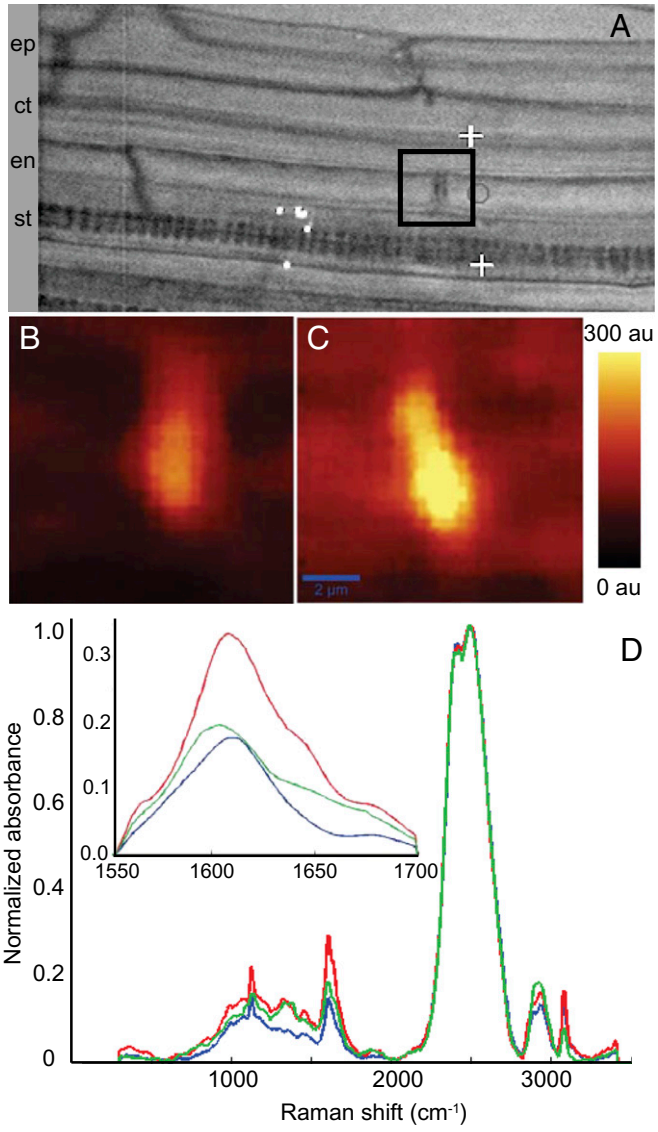

Fig. 4. Chemical imaging using Raman confocal microscope showing increased deposition of lignin at the disrupted Casparian strip in *esb1-1* mutant. (*A*) Representative image showing an endodermal cell junction used for acquiring 2D Raman spectra (marked with a black square box signifying a 10 × 10 μm^2 area). Raman images showing the modification of lignin deposition at the Casparian strip were obtained by integrating absorption intensities between 1,550 and 1,700 cm^{-1} in wild-type (*B*) and *esb1-1* (*C*). (*D*) Raman spectra extracted from the wild-type Casparian strip (blue), wild-type xylem (green), and *esb1-1* Casparian strip (red). *D Insert* shows the lignin spectra (1,550–1,700 cm^{-1}). Intensities were normalized to the peak height of D_2O at ~2,500 cm^{-1}, representing the O-D stretching band intensity. au, arbitrary units; ct, cortex; en, endodermis; ep, epidermis; st, stele.

From this evidence, we conclude that ESB1 is essential for the correct deposition of lignin-based Casparian strips and for their normal barrier function. In particular, ESB1 appears to be involved in the deposition of lignin patches that occurs early in the development of the Casparian strip (6) and also in the coalescence of these patches to form a continuous fine band of lignin as the Casparian strip matures. These conclusions are supported by the fact that ESB1 localization mirrors this coalescence process (Fig. 2), and in the absence of ESB1, malformed lignin patches form that fail to coalesce into a mature Casparian strip (Fig. 3). Lignin polymerization in the corners of cells in the *esb1-1* mutant (Fig. 3) may represent a default pathway that occurs when coalescence of the equatorial lignin patches is blocked. The CASP complex likely scaffolds the machinery for the precise localization of the lignification required to create the Casparian strip. This machinery includes ESB1 and the NADPH oxidase/peroxidase required for monolignol activation (6). During the initial development of the Casparian strip, this machinery occurs as equatorially located islands that produce patchy lignifications (6, 7). As Casparian strip development continues, these assembly islands coalesce, perhaps through the delivery of ESB1 and other components through cellular trafficking pathways, to eventually form a continuous strip. As functional units of this machinery are assembled, new lignin is laid down, bridging the gap between the initial lignin islands to finally form a precisely deposited lignin band sealed to the plasma membrane and spanning the cell walls of adjacent endodermal cells.

Importantly, the localization of ESB1 to the correct position in the cell wall for formation of the Casparian strip requires the function of the CASPs. The loss of ESB1 localization to the Casparian strip in the *casp1-1casp3-1* mutant (Fig. S1) could therefore account for the *casp1-1casp3-1* phenotypes, which show similar defects to *esb1-1* in both the morphology (7) and function of Casparian strips (Fig. 3 and Movie S1). Interestingly, we also observe that ESB1 is required for the correct localization of CASP1-GFP to the plasma membrane (Fig. S4). In the absence of ESB1, the localization of CASP1-GFP appears to stall at the "string-of-pearls" stage (7) with CASP1-GFP remaining localized in patches that do not coalesce into a mature Casparian strip domain.

Although its role in building Casparian strips is clear, the biochemical function of ESB1 remains obscure. When tested, dirigent proteins lack oxidative activity (12). However, in vitro in the presence of an oxidase, a dirigent protein has been shown to be able to direct the stereoselective coupling of the monolignol coniferyl alcohol to form the dimeric lignan pinoresinol (12). In this assay, the dirigent protein played no catalytic role in coupling but it was proposed to "bind and orientate" the monolignol before coupling (12). In vitro recombinant ESB1 in the presence of a fungal laccase appears to lack the capacity for stereoselective coupling of coniferyl alcohol to produce the dimeric lignin pinoresinol, although other potential monomers such as sinapyl alcohol and ρ-coumaryl alcohol were not tested (16). In the absence of any known activity for ESB1, its biochemical function remains speculative. It is possible that ESB1 plays a role in locating the lignin polymer of the Casparian strip by nucleating lignin polymerization at specified sites, and this suggestion is supported by the colocalization of ESB1 and the Casparian strip. Given the requirement of ESB1 for the correct localization of the CASPs, it is also possible that ESB1 has a role in bridging between the plasma membrane Casparian strip domain and lignin to allow a tight seal between the Casparian strip and the plasma membrane. Further experiments are required to test these hypotheses.

In wild-type plants suberin, a waxy material composed of both polyaliphatic and polyaromatic domains (17), is deposited between the plasma membrane and cell wall of endodermal cells in mature regions of the root. These suberin deposits are thought to act as an extracellular barrier to water and solutes (17). It is now clear that in *esb1*, suberin is ectopically deposited in endodermal cells close to the root tip, a region that is normally not suberized, and where Casparian strips first develop (2). This ectopic deposition can be clearly seen as alternating light and dark bands of suberin lamellae between the plasma membrane and cell wall (Fig. 5 *A–C*). The presence of suberin closer to the root tip in *esb1-1* can also be quantified by counting the first appearance of endodermal cells stained with Fluorol yellow, a suberin staining fluorescent dye (Fig. 5*E*). In addition, *esb1-1* lacks the unsuberised passage cells normally observed in more mature regions of the root (Fig. 5 *F* and *G*), suggesting that suberin is also ectopically deposited in these cells. Endodermal passage cells are thought to be specialized for ion transport in more mature regions of the root where suberin deposition blocks transport in normal endodermal cells (18). We observe a similar ectopic deposition of suberin in the *casp1-1casp3-1* double mutant (Fig. 5 and Fig. S5), consistent with the loss of ESB1 from the Casparian strip in this double mutant. Additionally, ectopic suberin deposition in *esb1-1* and *casp1-1casp3-1* also correlates with similar changes in the mineral nutrient composition of the leaves of both mutants, with significant reductions in the concentration of magnesium, calcium (strontium chemical analog), manganese, and iron, and increases in sulfur, potassium (rubidium chemical analog), and molybdenum (Dataset S1). Because suberin lamellae are deposited between the plasma membrane and the cell wall, they potentially limit transmembrane transport into cells, but are unable to block diffusion between cells in the cell wall. This function is unlike Casparian strips that span the cell wall and effectively block apoplastic transport. Suberin lamellae and Casparian strip formation at the endodermis are therefore expected to have different effects on nutrient uptake by roots. In *esb1*, both processes are affected together, revealing a fascinating interaction and providing an important tool to understand root function.

We propose that the ectopic deposition of suberin in *esb1-1* is a consequence of the defect in Casparian strip formation, revealing an intriguing cross-talk between formation of lignin and suberin-based cell wall modifications. The existence of such a mechanism is supported by the observation that in wild-type roots, suberin deposition occurs in a pocket of endodermal cells surrounding the developing lateral root primordium (19), and this deposition is congruent with the primordium penetrating the endodermis and disrupting the Casparian strip network (20). This knowledge raises the intriguing possibility that the ectopic deposition of suberin in *esb1* is being driven by a cell wall surveillance system normally responsible for coordinating the deposition of suberin as Casparian strips are disrupted during lateral root emergence. Surveillance systems that monitor primary cell walls has been reported. For example, the lack of cellulose synthesis in the *cesa* mutants initiates ectopic deposition of lignin (21, 22), and this response appears to be mediated by the plasma membrane bound receptor-like kinase THESEUS1 (23).

In conclusion, our analysis indicates that the dirigent domain containing protein ESB1 plays an essential role in building the extracellular lignin-based Casparian strip in endodermal cells of *A. thaliana* roots. ESB1 requires the CASP complex for its correct localization to the region of the cell wall where Casparian strips form, because the *esb1-1* knockout phenocopies *casp1-1casp3-1*. However, ESB1 is also required for the coalescence of the CASP complex into the continuous Casparian strip domain that underlies the Casparian strip. In the absence of ESB1, the barrier function of Casparian strips is impaired, causing ectopic deposition of suberin lamellae between the plasma membrane and the cell wall in both endodermal cells close to the root tip and endodermal passage cells. Such ectopic suberin deposition

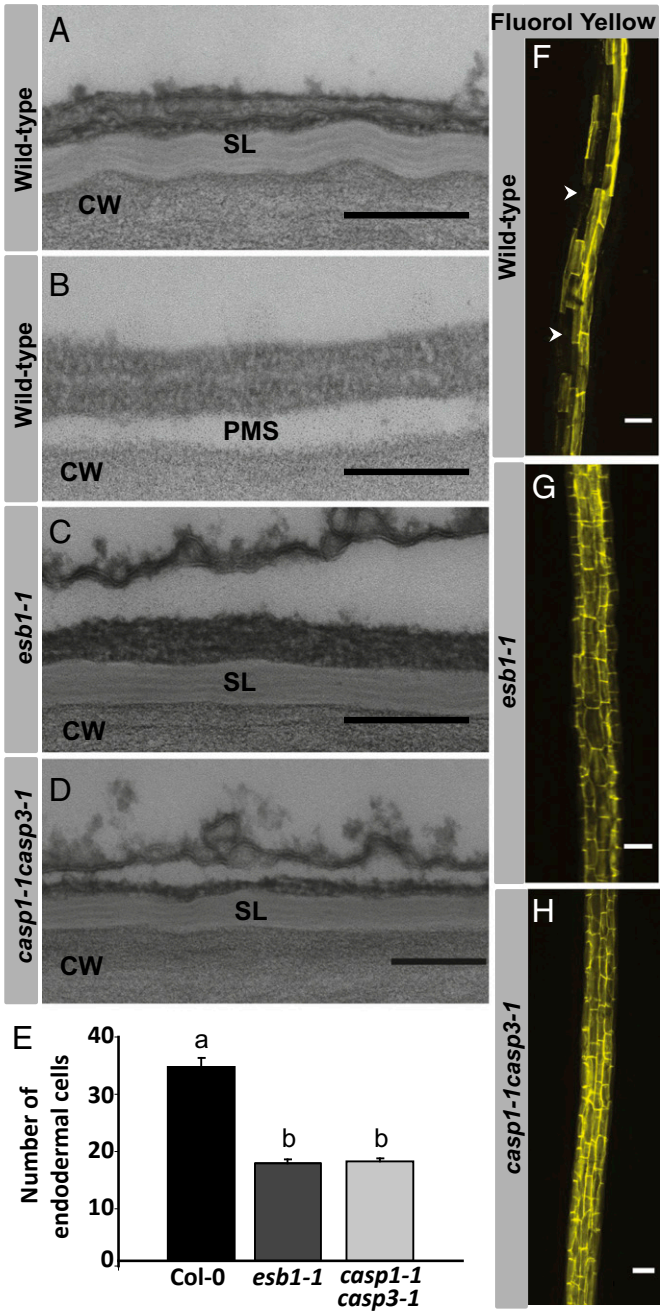

Fig. 5. Disruption of the Casparian strip through loss of *ESB1* function leads to ectopic deposition of suberin lamellae closer to the root tip and around passage cells in the endodermis. Transmission electron micrographs at periclinal wall of endodermal cells in wild-type mature region (*A*), wild-type young region (*B*), *esb1-1* young region (*C*), and *casp1-1casp3-1* young region (*D*). (*F–H*) Suberin deposition in roots detected by Fluorol Yellow staining of wild-type (*F*), *esb1-1* (*G*), and *casp1-1casp3-1* (*H*). Counting of the number of endodermal cells from the first fully expanded cell shows the early appearance of suberin in both *esb1-1* and *casp1-1casp3-1* double mutant compared with the wild type, with Fluorol yellow staining starting at the 17th endodermal cell after onset of elongation in *esb1-1*, and *casp1-1casp3-1* compared with the 33rd endodermal cell in wild-type (*E*). Different letters (a and b) indicate statistically significant differences between means by one-way analysis of variance (ANOVA) with Tukey–Kramer separation of means ($P < 0.05$), $n = 15$ roots. Arrowheads represent unsuberised passage cells. CW, cell wall; PMS, space generated by plasmolysis; SL, suberin lamellae. (Scale bars: *A–D*, 200 nm; *F–H*, 50 μm.)

reveals cross-talk between Casparian strips and suberin biosynthesis and suggests the existence of a cell wall surveillance system capable of perceiving the integrity of Casparian strips. The ectopically deposited suberin in *esb1-1* likely blocks transmembrane uptake of calcium and other ions into endodermal cells, limiting xylem loading and causing the reduction in leaf calcium and other minerals observed in plants with a disrupted ESB1 function. Our discoveries start to dissect the molecular mechanisms involved in endodermal control of solute entry into plants. Further, we provide in vivo evidence for proteins in the dirigent family functioning as part of the machinery that builds extracellular lignin-based structures, opening an avenue to determine the elusive role of this protein family *in planta*.

Methods

Plant Materials. *A. thaliana* Col-0 wild-type seeds were purchased from Lehle Seeds. The mutant *esb1-1* was identified in an ionomics screen of fast neutron mutagenized plants and was twice backcrossed to wild-type Col-0 (8, 9). The *casp1-1casp3-1* was generated by Roppolo et al (7).

Plant Growth Conditions. Plants were grown on agar solidified half-strength Murashige and Skoog (Caisson Laboratories) (24) with 1% sucrose (wt/vol) in sterile square (100 × 15 mm) Petri dishes (BD Falcon). Seeds were surface sterilized (10% bleach/0.1% Tween20 and 70% ethanol treatments), washed six times with sterile 18 MΩ H_2O and stratified for 3 d at 4 °C in 0.1% agarose solution. Petri dishes were kept in a growth room at 16-h light (90 μmol $m^{-2}·s^{-1}$): 8-h dark at a temperature of 19 °C to 22 °C. Plants were grown for either 7 or 14 d as required.

Elemental Analysis. Shoots of plants grown on agar plates were harvested into labeled Pyrex digestion tube (16 × 100 mm) sets by using surgical knife, plastic forceps, Teflon rod, and a beaker filled with 18 MΩ water. The tissues were dried in an oven at 88 °C for 20 h. Seven samples of the shoots were weighed (these were used to calculate the weights of all of the others on the basis of their averaged elemental concentrations; ref. 9). Concentrated nitric acid (0.7 mL per tube) (Trace metal grade; T.J. Baker) with indium internal standard (20 ppb) was added and samples digested at 115 °C for 5 h by using digital dry block heaters inside a fume hood. The acid-digested samples were diluted to a final volume of 6 mL with 18 MΩ water. Aliquots were transferred from the digestion tubes into 96-well deepwell plates for analysis. Elemental analysis was performed on an ICP-MS (inductively coupled plasma mass spectrometry) (Elan DRC II; PerkinElmer) equipped with Apex sample introduction system and SC-2 autosampler (Elemental Scientific). Twenty elements (Li, B, Na, Mg, P, S, K, Ca, Mn, Fe, Co, Ni, Cu, Zn, As, Se, Rb, Sr, Mo, Cd) were monitored; their concentrations were obtained by using calibration standards with blanks and the external calibration method of the Elan software (version 3.4). Normalized concentrations of the samples were obtained by using the solution concentrations and the calculated weights (9).

Plasmid Construction and Transformation. The −2,245-bp region from the first ATG was used as the promoter for construction of the *pESB1::ESB1::mCherry* construct. Genomic DNA was amplified (forward primer 5′-CACCCAACAATGAGGACACTGAGC-3′ and reverse primer 5′-GTAAGAAAGATAAACGGTAC-3′. mCherry was amplified (forward primer 5′-GTTGTTGAGTGTACCGTTTATCTTTCTTACGGAGGAGGAGGAGCTATGGTGAGCAAGGCGAGGA-3′ and reverse primer 5′-TCACTTGTACAGCTCGTCCATGC-3′). The amplified DNA fragment from genomic DNA and mCherry was fused by fusion PCR (forward primer 5′-GAGAATTCCAACAATGAGGACACTGAGC-3′ and reverse primer 5′- GAGCTCGAGTCACTTGTACAGCTCGTCCATGC-3′). The resulting fused fragment was digested with EcoRI and XhoI and cloned into the EcoRI and XhoI site of pENTR2B Dual Selection Vector (Invitrogen) followed by the destination vector GWB510 (25) by using LR Clonase (Invitrogen). The −1,172-bp region from the first ATG of *ESB1* was used for complementation of *esb1-1* with wild-type *ESB1*. Genomic DNA was amplified (forward primer 5′- AAAATATTTCTTCTAAATTTATTGAGAATCCATACGAT -3′ and reverse primer 5′- TCTACGTCTCTTTTTATTGTAGAAAATTTTAATCTGC -3′) with gateway adapters and recombined into pDONR 221 by using BP clonase enzyme (Invitrogen). The resulting entry clone was recombined with the promoterless binary destination vector pCC1136 by using LR Clonase (Invitrogen). All constructs were transformed into electro competent *Agrobacterium tumefaciens* GV3101 cells. Positive clones were selected by using suitable antibiotic resistance and used for plant transformation by using the floral dip method (26). Plants were selected by using resistance to glufosinate-ammonium (Basta) in soil. We note

that ESB1 used in the mCherry experiment contained a mutation (Ala^{137}, which is not conserved among ESB1 homologs, is substituted with Thr) because we could not obtain nonmutated ESB1. Although ESB1-mCherry in this work has the mutation, the construct fully complemented the *esb1-1* mutant (Fig. S3), indicating that the protein activity of ESB1 is the same as that of wild-type ESB1.

Optical Microscopy. Autofluorescence of the Casparian strip was observed on cleared roots (27) by using a Zeiss LSM700 confocal microscopy. Briefly, 5- to 6-d-old seedlings (Col-0, *esb1-1*, and *casp1-1casp3-1*) were transferred to a Petri dish containing 0.24 M HCl and 20% methanol and incubated for 15 min at 57 °C. The solution was replaced with 7% NaOH and 60% ethanol and incubated for 15 min at room temperature. After these clearing steps, roots were rehydrated at room temperature by sequential replacement of the solution using 40% ethanol for 5 min, 20% ethanol for 5 min, 10% ethanol for 5 min, 5% ethanol for 15 min, and finally 25% glycerol was added. For mounting root on glass slides, 50% glycerol was used. Cleared roots were visualized for autofluorescence with excitation at 488 nm and with band path filter of 500–600 nm. *Z*-stack images were obtained by imaging several slices with 0.95 μm thickness. Fluorol yellow was detected with a standard GFP filter under a wide-field microscope (Leica DM5500). Fluorol yellow staining was performed as described (28). For assay of the apoplastic barrier, seedlings were incubated in the dark for 10 min in a fresh solution of 15 μM (10 μg/mL) PI and rinsed twice in water (29). For quantification, "onset of elongation" was defined as the point where an endodermal cell in a median optical section was more than twice its width. From this point, cells in the file were counted until the respective signals were detected (27).

Electron Microscopy. The state I endodermis was visualized by using root sections taken 6 mm from the root tip. The state II endodermis was visualized by using root sections taken at the mature region of the root (in the region of the root where lateral roots start to develop) ∼30 mm from the root tip in 14-d-old seedling. Transmission electron microscopy (TEM) was conducted by using a described protocol (30). Ultrathin sections were prepared by using a microtome from London resin white-embedded samples. Samples were visualized with an FEI/Philips CM-10 transmission electron microscope (FEI Company) at an accelerating voltage of 80 kV.

Immunogold Labeling. Subcellular localization was performed by using transmission electron microscopy (TEM) after immunogold labeling of root sections taken 6 mm from the root tip in 7-d-old *A. thaliana* seedlings grown in plates on agar solidified medium. Ultrathin section were prepared from London resin white-embedded root samples and transferred on to nickel grids (Electron Microscopy Science). After transfer immunocytochemistry (ICC) was performed by using standard procedures (30). ICC involved the anti-ESB1 primary antibody with a dilution of 1:250 in Tris-buffered saline (TSB) containing 0.5% bovine serum albumin (TSB-B) overnight and secondary antibody goat anti-rabbit IgG EM grade 10 nm gold conjugate (Ted Pella) at a 1:50 dilution in TBS containing 0.5% Tween-20 and 1% BSA (TBS-TB). Samples were stained with 2% uranyl acetate in 70% methanol for 10 min. Custom affinity-purified polyclonal anti-ESB1 antibodies were made by Genscript USA and were used as a primary antibody. Anti-ESB1 antibodies were generated in rabbits against a synthetic peptide (CGTQQNQPHQFTDGL) designed from the C terminus of the ESB1 protein. Root sections were visualized with an FEI/Philips CM-10 transmission electron microscope (FEI Company) by using an accelerating voltage of 80 kV.

Raman Confocal Microscopy. Confocal Raman microscopy was performed for lignin imaging by using a described method (15) on cleared root samples. After clearing, roots were suspended and subsequently mounted in deuterium oxide. Two-dimensional Raman spectra were obtained by using a confocal Raman microscope (WITec CRM200) for chemical imaging with a 50× objective and a 514 nm polarized light source. Using a piezoelectric scan stage, spectral data were acquired every 200 nm. Images were obtained by using an integration time of 1 s for each spectrum. Image analysis was performed by using the WITec project software (version 1.88). Different spectral map intensities were normalized by using the reference peak (oxygen-deuterium stretching band ∼2,500 cm^{-1}) using a Raman spectrum processing program (31).

ACKNOWLEDGMENTS. We thank Dr. Charles Daghlian (Dartmouth College Microscopy Facility), Dr. Aaron Taylor (Purdue University Bioscience Imaging Facility), and the University of Aberdeen and University of Lausanne for technical support. This work was supported by grants from the US National Science Foundation Arabidopsis 2010 Program to D.E.S and M.L.G (Award IOB 0419695), the European Commission Marie Curie Career Integration to D.E.S. (Award FP7-PEOPLE-2011-CIG), and the Japan Society for the Promotion of Science (T.K.).

1. Steudle E (2001) The cohesion-tension mechanism and the acquisition of water by plant roots. *Annu Rev Plant Physiol Plant Mol Biol* 52:847–875.
2. Naseer S, et al. (2012) Casparian strip diffusion barrier in Arabidopsis is made of a lignin polymer without suberin. *Proc Natl Acad Sci USA* 109(25):10101–10106.
3. Steudle E (2000) Water uptake by plant roots: An integration of views. *Plant Soil* 226: 45–56.
4. White PJ (2001) The pathways of calcium movement to the xylem. *J Exp Bot* 52(358): 891–899.
5. Geldner N (2013) The endodermis. *Annu Rev Plant Biol* 64:531–558.
6. Lee Y, Rubio MC, Alassimone J, Geldner N (2013) A mechanism for localized lignin deposition in the endodermis. *Cell* 153(2):402–412.
7. Roppolo D, et al. (2011) A novel protein family mediates Casparian strip formation in the endodermis. *Nature* 473(7347):380–383.
8. Baxter I, et al. (2009) Root suberin forms an extracellular barrier that affects water relations and mineral nutrition in Arabidopsis. *PLoS Genet* 5(5):e1000492.
9. Lahner B, et al. (2003) Genomic scale profiling of nutrient and trace elements in Arabidopsis thaliana. *Nat Biotechnol* 21(10):1215–1221.
10. Ranathunge K, Schreiber L (2011) Water and solute permeabilities of Arabidopsis roots in relation to the amount and composition of aliphatic suberin. *J Exp Bot* 62(6): 1961–1974.
11. Finn RD, et al. (2010) The Pfam protein families database. *Nucleic Acids Res* 38(Database issue):D211–D222.
12. Davin LB, et al. (1997) Stereoselective bimolecular phenoxy radical coupling by an auxiliary (dirigent) protein without an active center. *Science* 275(5298):362–366.
13. Davin LB, Lewis NG (2000) Dirigent proteins and dirigent sites explain the mystery of specificity of radical precursor coupling in lignan and lignin biosynthesis. *Plant Physiol* 123(2):453–462.
14. Ralph J, et al. (2009) Lignification: Are lignins biosynthesized via simple combinatorial chemistry or via proteinaceous control and template replication? *Rec Adv Polyphen Res* 1:36–66.
15. Schmidt M, Perera P, Schwartzberg AM, Adams PD, Schuck PJ (2010) Label-free in situ imaging of lignification in plant cell walls. *J Vis Exp* (45):2064.
16. Kim KW, et al. (2012) Opposite stereoselectivities of dirigent proteins in Arabidopsis and schizandra species. *J Biol Chem* 287(41):33957–33972.
17. Franke R, Schreiber L (2007) Suberin—a biopolyester forming apoplastic plant interfaces. *Curr Opin Plant Biol* 10(3):252–259.
18. Peterson CA, Enstone DE (1996) Functions of passage cells in the endodermis and exodermis of roots. *Physiol Plant* 97:592–598.
19. Martinka M, Dolan L, Pernas M, Abe J, Lux A (2012) Endodermal cell-cell contact is required for the spatial control of Casparian band development in Arabidopsis thaliana. *Ann Bot (Lond)* 110(2):361–371.
20. Lucas M, et al. (2013) Lateral root morphogenesis is dependent on the mechanical properties of the overlaying tissues. *Proc Natl Acad Sci USA* 110(13):5229–5234.
21. Caño-Delgado AI, Metzlaff K, Bevan MW (2000) The eli1 mutation reveals a link between cell expansion and secondary cell wall formation in Arabidopsis thaliana. *Development* 127(15):3395–3405.
22. Caño-Delgado A, Penfield S, Smith C, Catley M, Bevan M (2003) Reduced cellulose synthesis invokes lignification and defense responses in Arabidopsis thaliana. *Plant J* 34(3):351–362.
23. Hématy K, et al. (2007) A receptor-like kinase mediates the response of Arabidopsis cells to the inhibition of cellulose synthesis. *Curr Biol* 17(11):922–931.
24. Murashige T, Skoog F (1962) A revised medium for rapid growth and bio assays with tobacco tissue cultures. *Physiol Plant* 15:473–497.
25. Nakagawa T, et al. (2007) Improved Gateway binary vectors: High-performance vectors for creation of fusion constructs in transgenic analysis of plants. *Biosci Biotechnol Biochem* 71(8):2095–2100.
26. Clough SJ, Bent AF (1998) Floral dip: A simplified method for Agrobacterium-mediated transformation of Arabidopsis thaliana. *Plant J* 16(6):735–743.
27. Malamy JE, Benfey PN (1997) Organization and cell differentiation in lateral roots of Arabidopsis thaliana. *Development* 124(1):33–44.
28. Lux A, Morita S, Abe J, Ito K (2005) An improved method for clearing and staining free-hand sections and whole-mount samples. *Ann Bot (Lond)* 96(6):989–996.
29. Alassimone J, Naseer S, Geldner N (2010) A developmental framework for endodermal differentiation and polarity. *Proc Natl Acad Sci USA* 107(11):5214–5219.
30. Kolosova N, Sherman D, Karlson D, Dudareva N (2001) Cellular and subcellular localization of S-adenosyl-L-methionine:benzoic acid carboxyl methyltransferase, the enzyme responsible for biosynthesis of the volatile ester methylbenzoate in snapdragon flowers. *Plant Physiol* 126(3):956–964.
31. Reisner LA, Cao A, Pandya AK (2011) An integrated software system for processing, analyzing, and classifying Raman spectra. *Chemometr Intell Lab* 105:83–90.